Characterization of low temperature GaAs antenna array terahertz emitters

M. Awad,[a] M. Nagel, and H. Kurz
Institut für Halbleitertechnik, RWTH Aachen University, Sommerfeldstr. 24, 52074 Aachen, Germany

J. Herfort and K. Ploog
Paul-Drude-Institut für Festkörperelektronik, Hausvogteiplatz 5-7, 10117 Berlin, Germany

(Received 25 June 2007; accepted 1 October 2007; published online 2 November 2007)

We present a fabrication concept for photoconductive terahertz antenna arrays based on substrate-transferred thin films of low-temperature-grown GaAs semiconductor material. Adjacent array elements are physically decoupled by removing completely the photoconductive material in between. In contrast to former array devices based on intrinsic bulk GaAs substrates, this method allows the use of arbitrary carrier substrates with enhanced transmission properties. The emission characteristics of the device are investigated in terms of bandwidth, directivity, and saturation caused by charge-carrier induced field-screening effects. Screening-free operation is experimentally observed for an average optical power density below 2.2×10^{-4} mW/μm^2. © *2007 American Institute of Physics*. [DOI: 10.1063/1.2800885]

Photoconductive metal-semiconductor-metal (MSM) structures such as coplanar strip lines or dipole antennas are still the most common devices for terahertz signal generation based on femtosecond laser oscillator sources with pulse energies in the nanojoule range. At high excitation densities, the MSM terahertz sources' efficiency, however, suffers considerably from space charge and radiation field screening of the bias field.[1] A way to improve the efficiency of photoconductive terahertz devices is to increase the active area, thereby reducing the excitation density incident onto the device. These large aperture devices, however, require high bias voltages in the kilovolt range. Alternatively, it is possible to fabricate a terahertz emitter with a large effective aperture, consisting of periodically spaced MSM elements, and thus reduce the required bias voltages from kilovolts to tens of volts, depending on the width of MSMs' photoconductive gap. Such a device based on semi-insulating GaAs has recently been demonstrated.[2]

In this work, we demonstrate an alternative fabrication concept for terahertz antenna arrays based on substrate-transferred thin films of low-temperature (LT) grown GaAs semiconductor material. The epitaxial lift-off method[3] allows the use of LT-GaAs films on arbitrary carrier substrates with enhanced transmission properties at optical and terahertz frequencies in comparison to intrinsic GaAs, which is known to exhibit considerable attenuation and dispersion at terahertz frequencies.[4] As opposed to semi-insulating (SI) GaAs, LT GaAs has the very important advantage of short carrier lifetime[5] on the order of 150 fs allowing the device to be used interchangeably as an emitter, detector, and under impulsive or cw optical excitation. The latter excitation method has recently been discussed for terahertz array devices by Saeedkia *et al.*.[6] Furthermore, the higher breakdown field for LT GaAs (~500 kV/cm) permits the application of greater electric fields in comparison to SI GaAs (10–100 kV/cm).[7] Therefore, LT GaAs is considered to be one of the best materials for photoconductive terahertz devices.[8]

In the following, the fabrication process of the antenna array devices is described. In the first step, two sets of 14 interdigitated 4 μm wide electrodes are deposited on top of a lattice-matched layer system consisting of 150 nm SI GaAs, a 100 nm AlAs layer, followed by a 1.3 μm layer of LT GaAs grown using molecular beam epitaxy onto a [100] oriented SI GaAs substrate. The electrode patterning method used for this step is photolithography using AZ5214 photoresist followed by metal layer deposition (Ti/Au, 10/200 nm) and subsequent lift-off in acetone. In a further photolithography step, the array structure is selectively masked with a photoresist layer. Next, the exposed LT-GaAs areas are etched away by chemical wet etching in a H_2O_2:H_2SO_4:H_2O (8:1:1) solution giving access to the AlAs layer. Finally, the AlAs sacrificial layer is etched off completely in a 10% HF solution yielding a self-contained, freestanding LT-GaAs chip carrying the antenna structure, shown in Fig. 1(a). The terahertz array chip is then transferred to a 500 μm thick, optically and terahertz transparent sapphire substrate. As shown in the cross-sectional view in Fig. 1(b), the photoconductive gap between the electrodes comprising each array element is 11 μm wide, while consecutive array elements are separated by a distance of 4 μm. For the proper operation of the device, it is important to

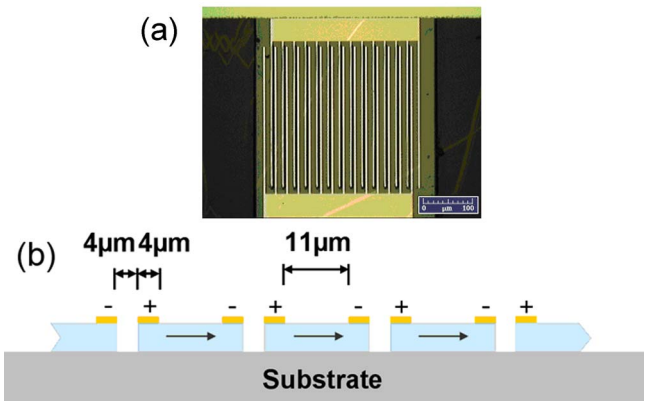

FIG. 1. (Color online) (a) Micrograph of terahertz array antenna device. (b) Cross-sectional view of terahertz antenna array.

[a]Author to whom correspondence should be addressed; electronic mail: awad@iht.rwth-aachen.de

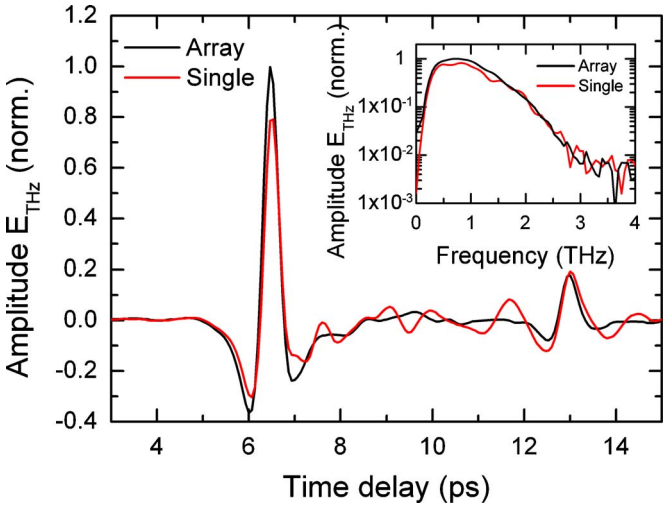

FIG. 2. (Color online) Time-resolved scans of terahertz pulse for array emitter (dark line) and single element (light line) and their respective spectra in inlay.

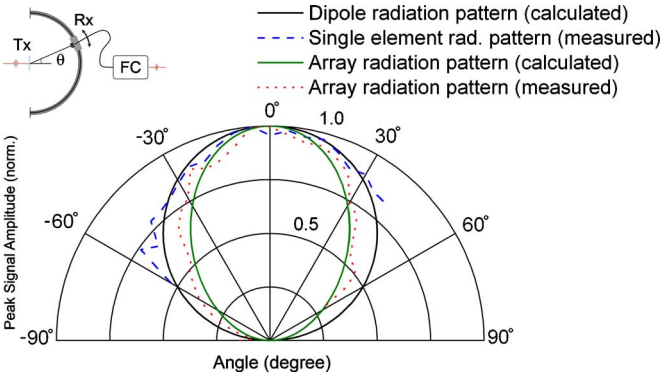

FIG. 3. (Color online) Calculated radiation pattern for dipole (black solid line) and measured single element radiation pattern (dashed line). Array radiation pattern calculated based on array theory (light solid line) and measurement (dotted). Inlay: experimental setup with fiber coupled and dispersion compensated (FC) receiver for radiation pattern measurement.

ensure that no semiconductor material is left between adjacent elements, since radiative contributions from these areas would destructively interfere. Also, having the interelement area void from any semiconductor material reduces the device dark current by at least 50%.

To measure the emitted terahertz field from a single array element and a fully illuminated array, the device is placed in a standard confocal terahertz-time-domain spectroscopy system and excited with optical pulses from a mode-locked Ti:sapphire laser, operating at 780 nm with a repetition rate of 76 MHz and 100 fs pulse width. The emitter is mounted such that the LT-GaAs chip directly faces the optical excitation, while the terahertz radiation is coupled out through the sapphire substrate facing the detector. For all measurements, no emitter-side substrate lens is used. The antenna array is biased with a 1.1 kHz, 0–40 V amplitude square wave, which also provides the reference for lock-in detection. As a detector, a 20 μm dipole antenna with a 5 μm photoconductive gap is used. A 3 mm diameter silicon substrate lens placed on the back side of the detector focuses the terahertz radiation onto the photoconductive gap. A current amplifier connected to the dipole antenna converts the induced signal current into a voltage which is detected by a lock-in amplifier.

For the first measurement, the optical beam with 5.5 mW power is focused onto a single element at the center of the array illuminating an active area of approximately 95 μm^2. A second measurement is performed under the same bias conditions, but with the optical beam fully illuminating the array covering an active area of 4.3×10^4 μm^2. In both cases, identical photocurrents of 1.3 μA are observed. Hence, without the influence of parasitic effects, identical terahertz field amplitudes should be observed for single emitter and full array excitation since the generated terahertz field amplitude $E_{\text{terahertz}}(t)$ is proportional to $(\partial/\partial t)j(t)$, with j being the photocurrent density. Time-resolved scans and their respective amplitude spectra shown in Fig. 2, however, reveal an approximately 30% increase in signal amplitude between the fully illuminated array and single element excitation.

To investigate the origin of the increase in emitted terahertz radiation observed in Fig. 2, we measure the directivity dependence on the optical excitation area. A more strongly directed terahertz beam will translate into a larger terahertz amplitude at the detector due to a higher amount of radiation that is collected at the finitely sized mirrors used in the measurement setup. In order to determine the directivity for both single element and fully illuminated array excitation cases, the radiation pattern is mapped with a further setup, depicted in the inlay in Fig. 3. As shown, the antenna array is placed at the center of a rotation stage. The same terahertz detector as was used in the previous measurement is coupled to a 1 m long optical fiber and mounted on a rotation stage. A grating pair is used to compensate for the dispersion in the fiber. Two sets of measurements are acquired as before. For the first measurement, the optical beam is focused onto a single array element. The measured radiation pattern, plotted in Fig. 3 (dashed line), matches very well with the radiation pattern of a dipole (dark solid line). With the entire array illuminated, the radiation pattern, as expected, shows a narrower beam width due to the larger number of excited antenna elements. The light solid line in Fig. 3 shows the calculated normalized radiation pattern for a 14 element array with uniform excitation based on array theory.[9] Since the element spacing l is much smaller than the center terahertz wavelength $l \ll \lambda_{\text{terahertz}}$, we do not observe the high gain and directivity attainable using a typical array configuration with l in the order of $\lambda_{\text{terahertz}}$. However, the measured array radiation pattern, Fig. 3 (dotted line), fits qualitatively well to the analytical model described by array theory. It should be considered that, the applied excitation spot is not uniform (as considered for the calculation).The observed radiation angles for single element and array emitter are approximately 120° and 90° (both full width at half maximum), respectively. Accounting for the finitely sized collecting terahertz mirrors used in the experimental setup, having an aperture angle of 30°, the observed increase of 30% in signal amplitude at low pump power can indeed be largely attributed to the enhanced directivity of the array.

At higher optical pumping levels, however, screening effects are expected to become increasingly relevant. To investigate this regime, we further compare the emitted terahertz peak amplitudes at increased optical excitation power P_{NIR} for both cases. In Fig. 4, the measured terahertz peak amplitude, $E_{\text{terahertz}}(P_{\text{NIR}})$, of the array emitter versus optical excitation is plotted. In the case of negligible screening, a linear

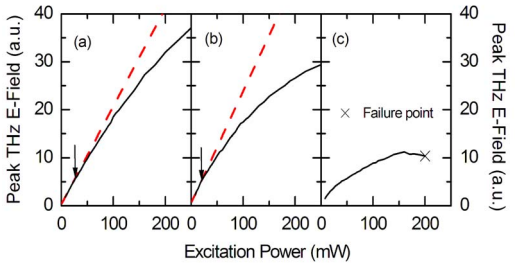

FIG. 4. (Color online) Saturation curve for (a) single element (focused optical spot, *X* marks failure point of the device), (b) reference excitation spot (spot size adjusted to maximize terahertz amplitude at low excitation power), and (c) array with large excitation spot compared to reference spot (spot size adjusted to maximize terahertz amplitude at high excitation power).

increase of $E_{\text{terahertz}}(P_{\text{NIR}})$ is expected. Recently, Kim and Citrin[1] theoretically investigated the saturation behavior of single element GaAs terahertz emitters due to Coulomb screening and back action of the radiated terahertz field. In their work, excitation intensities I_{NIR} below approximately 6×10^{-4} mW/μm^2 were identified to be desirable to avoid screening related emitter degradation. Here, the single emitter is pumped with intensities I_{NIR} (or corresponding P_{NIR}) between 7.9×10^{-2} mW/μm^2 (7.5 mW) and 2.1 mW/μm^2 (200 mW). Consequently, for the single element, a linear regime of $E_{\text{terahertz}}$ (P_{NIR}) cannot be identified in Fig. 4(a). At about 1.63 mW/μm^2 (155 mW), complete saturation occurs. The device finally fails at an excitation intensity of 2.1 mW/μm^2. Figure 4 also shows two further graphs of the emitted terahertz radiation from a fully illuminated array structure with two different illumination spot sizes. The data represented by Fig. 4(b) were acquired using a reference spot size, adjusted to maximize the emitted terahertz signal in the regime of negligible screening at $I_{\text{NIR}}=8.3\times10^{-5}$ mW/μm^2. In this case the excitation spot area approximately equals the total array area. A linear increase of $E_{\text{terahertz}}$ (P_{NIR}) is observed up to $I_{\text{NIR}}=2.2\times10^{-4}$ mW/μm^2 and $P_{\text{NIR}}=20$ mW, as indicated by the arrow. A further increase in excitation spot size beyond the reference spot size of Fig. 4(b), in the pump intensity regime where the influence of screening is noticeable ($I_{\text{NIR}}=2\times10^{-3}$ mW/μm^2), leads to an increase of the generated terahertz radiation. In this latter case, shown in Fig. 4(c), the device remains longer in a linear regime compared to the reference spot excitation in Fig. 4(b), up until $P_{\text{NIR}}=25$ mW. The intensity where $E_{\text{terahertz}}(P_{\text{NIR}})$ begins to diverge from linearity is $I_{\text{NIR}}=2.2\times10^{-4}$ mW/μm^2, the same value as determined in the previous case, shown in Fig. 4(b).

Considering a pulse energy density of 2.9 fJ/μm^2, an absorption coefficient $\alpha=12\,000$ cm^{-1}, and a refractive index $n=3.42$ for LT GaAs,[10] we infer a critical average photocarrier density of $\sim1.5\times10^{16}$ cm^{-3} above which screening effects become relevant. For the larger excitation spot size, an increased loss of optical excitation power outside the active area of the device is introduced. Therefore, the increase factor for the linear regime is considerably reduced for the larger excitation spot plotted in Fig. 4(c) in comparison to Fig. 4(b). However, at higher pump power, this loss of excitation beyond the array area is compensated for by the lower excitation density leading to increased emission efficiency. Due to power limitations of our laser source, we were not able to identify the power range where complete saturation of the fully illuminated array occurs. The maximum excitation power applied was 350 mW corresponding to an intensity of 2.8×10^{-3} mW/μm^2, which is almost three orders of magnitude below the intensity that was needed to completely saturate the single emitter. At 350 mW excitation power, the terahertz array antenna achieves a fivefold field amplitude increase in comparison to the maximum terahertz field generated by the single emitter.

Interestingly, terahertz radiation emitted from SI-GaAs based array structures[11] exhibited a strong blueshift of the generated terahertz spectrum for decreasing excitation spot sizes, with maximum emission for terahertz wavelengths in the range of the excitation spot diameter. In our case, however, we do not observe any significant frequency dependence on illumination spot size. Referring back to Fig. 2(a), the amplitude spectra of single emitter and array both peak at approximately 750 GHz, even in the case of the single emitter with an excitation spot diameter $d=10$ μm (array: $d=300$ μm), where d is much smaller than the generated terahertz wavelength $\lambda_{\text{terahertz}}$. We attribute this behavior to the improved electrodynamic decoupling of our array elements in comparison with SI-GaAs structures in Ref. 11 resulting from the lack of a metallic masking layer and semiconductor material in between elements. Therefore, in contrast to an aperture-like irradiation the behavior of our array is mainly determined by the radiation property of each array-embedded single element. Our results indicate also that the proposed antenna arrays can be further enhanced in terms of directivity and terahertz field amplitude by increasing the number of array elements and element separation distance.

In summary, we presented a terahertz antenna array device fabricated on LT GaAs using an epitaxial lift-off technique. Epitaxial lift-off allows added versatility in the choice of substrate, or even direct bonding onto integrated terahertz systems. We demonstrated that the terahertz antenna array can generate drastically increased terahertz field amplitudes compared to a single element and that even for high fluence, the array remains in an unsaturated region of operation, whereas the single element device is well beyond its failure limit.

The authors would like to acknowledge the Innovation Department of North Rhine Westphalia and the Federal Ministry of Education and Research (BMBF) for financial support.

[1] D. S. Kim and D. S. Citrin, Appl. Phys. Lett. **88**, 161117 (2006).
[2] A. Dreyhaupt, S. Winnerl, T. Dekorsy, and M. Helm, Appl. Phys. Lett. **86**, 121114 (2005).
[3] E. Yablonovitch, D. M. Hwang, T. J. Gmitter, L. T. Florez, and J. P. Harbison, Appl. Phys. Lett. **56**, 2419 (1990).
[4] C. J. Johnson, G. H. Sherman, and R. Weil, Appl. Opt. **8**, 1667 (1969).
[5] G. Segschneider, T. Dekorsy, H. Kurz, R. Hey, and K. Ploog, Appl. Phys. Lett. **71**, 2779 (1997).
[6] D. Saeedkia, R. R. Mansour, and S. Safavi-Naeini, IEEE Trans. Antennas Propag. **53**, 4044 (2005).
[7] J. K. Luo, H. Thomas, D. V. Morgan, D. Westwood, and R. H. Williams, Semicond. Sci. Technol. **9**, 2199 (1994).
[8] M. Tani, S. Matsuura, K. Sakai, and S. Nakashima, Appl. Opt. **36**, 7853 (1997).
[9] C. Balanis, *Antenna Theory*, 3rd ed. (Wiley-Interscience, Hoboken, NJ, 2005).
[10] P. Grenier and J. F. Whitaker, Appl. Phys. Lett. **70**, 1998 (1997).
[11] A. Dreyhaupt, S. Winnerl, M. Helm, and T. Dekorsy, Opt. Lett. **31**, 1546 (2006).